CROSS-CALIBRATION OF THE ROSETTA NAVIGATION CAMERA

Thiago Statella [1], Bernhard Geiger [2]

[1]Instituto Federal de Educação, Ciência e Tecnologia de Mato Grosso, Rua Zulmira Canavarro 95, 78032-175, Cuiabá-MT, thiago.statella@cba.ifmt.edu.br; [2]Aurora Technology B. V., Camino bajo del Castillo s/n, 28692 Villanueva de la Cañada, Madrid, Spain, bernhard.geiger@esa.int [3]

ABSTRACT

This publication describes the radiometric cross-calibration of NavCam with respect to OSIRIS NAC. We estimated the spectral radiance distribution over the OSIRIS filters by fitting an exponential curve to the average nucleus radiance as obtained by the OSIRIS NAC seven bands. From the OSIRIS spectral distribution we used the NavCam sensitivity curve to determine the average nucleus radiance in NavCam broad-band filter. The ratio between the average nucleus radiance and the average nucleus DN (Digital Number) produced the calibration factor which we needed to convert NavCam DN into radiance. The estimated radiometric factor was $(7.14 \pm 0.07) \cdot 10^{-7}$ and it is suited for processing images acquired with the attenuation filter (FOC_ATT) and HIGH gain mode. In order to check the results we applied that factor to an extended set of NavCam images and analyzed the average nucleus radiance as a function of the phase angle. We then confirmed the consistence of our method.

Key words *— 67P/Churyumov-Gerasimenko, photometry, comet, radiometric calibration.*

1. INTRODUCTION

In August 2014 the Rosetta spacecraft reached its target, the comet 67P/Churyumov-Gerasimenko. The mission was active until September 2016, when the spacecraft landed on the comet nucleus. The main scientific camera in the payload was the OSIRIS system [1][2], for which radiometric and geometric calibration had been performed. In addition to the suite of scientific instruments, Rosetta also carried an optical broad-band camera used for navigational purposes, named NavCam. Accurate geometric information was available or the navigational camera, but less effort was spent in its radiometric properties characterization. However, the NavCam draw the attention of the scientific community because a great amount of data was available, which could be used as complementary information for the OSIRIS data. Non-calibrated NavCam images were used for context images [3], and study of comet outbursts [4], for example.

In order to extract photometric properties of the 67P comet from NavCam images, the camera should be calibrated. In this paper, we present the results of the radiometric calibration of the NavCam based on radiance images of the OSIRIS Narrow Angle Camera (NAC), one of the two (the other being the Wide Angle Camera - WAC) scientific cameras onboard Rosetta. Currently, radiometric calibrated images acquired from the navigation camera are available and can be used for scientific purposes as well as the OSIRIS system.

2. CROSS-CALIBRATION OF THE NAVCAM

For the radiometric calibration we have considered a disk-integrated methodology using the average comet nucleus signal in the calculations. For that purpose, we extracted the Digital Number (DN) values of pixels laying in the comet nucleus with a binary mask for marking the nucleus limb.

The NavCam images used for this study have been acquired by Rosetta on 2014-08-01 in the time range from t=12:07:17h to t=21:07:17h. The data are available in ESA's Planetary Science Archive (PSA) as un-calibrated "Level 2" images in PDS3 format [5]. The set of eight available images is presented in Figure 1, which displays the original images, a zoomed insight of the comet nucleus (at the bottom left corner) and the binary mask used to segment the pixels of the nucleus (at the bottom right corner). Information about these images is given in Table 1. The integration time for all scenes was 1.0 s.

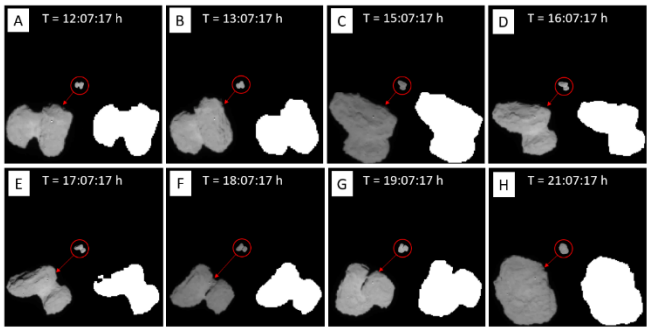

Figure 1. NavCam images acquired on 2014-08-01, at times ranging from t = 12:07:17h to t = 21:07:17h. Credits: ESA/Rosetta/NAVCAM. Archive dataset: [1].

Table 1. Information on NAVCAM images.

ID	Average signal [DN/s]	σ [DN/s]
ROS_CAM1_20140801T120717F.FIT	1876	±168
ROS_CAM1_20140801T130717F.FIT	1864	±153
ROS_CAM1_20140801T150717F.FIT	1764	±162
ROS_CAM1_20140801T160717F.FIT	1719	±225
ROS_CAM1_20140801T170717F.FIT	1759	±242
ROS_CAM1_20140801T180717F.FIT	1791	±210
ROS_CAM1_20140801T190717F.FIT	1787	±177
ROS_CAM1_20140801T210717F.FIT	1733	±125

As a pre-processing step, we have subtracted a bias field from each scene in order to correct the detector offset. Next, we have converted the images from DN count numbers to DN per second (DN/s) by dividing them by the respective scene exposure time. Binary masks for the comet nucleus have been created by using Otsu's algorithm [6] for automatic thresholding [7]. Next, morphological opening and closing transformations, which act as local adaptive filters, have been applied to the segmentation in order to filter out black and white isolated pixels caused by noise or artefacts during the acquisition process. Finally, a morphological erosion, which produces a shrinking effect on the brighter objects, has been applied to the masks for avoiding the influence of pixels in the fringe of the nucleus when calculating the average nucleus Digital Number per second (DN/s).

For the comparison we used OSIRIS-NAC images acquired on 2014-08-01 from t=11:50:14.576h to t=20:44:43.524h, which were radiometrically calibrated as described by [8]. The calibrated images are available as "Level 3" datasets in the Planetary Science Archive [9]. Figure 2 shows the average comet nucleus spectral radiance L_λ (in $Wm^{-2}sr^{-1}nm^{-1}$) and the vertical bars stand for its standard deviation. There are 8 sets of OSIRIS images which are each composed of 7 scenes acquired in different filters: Blue, Green, Orange, Hydra, Red, Near Infrared (NIR) and Infrared (IR). The procedure to create the masks is the same as used for NavCam images.

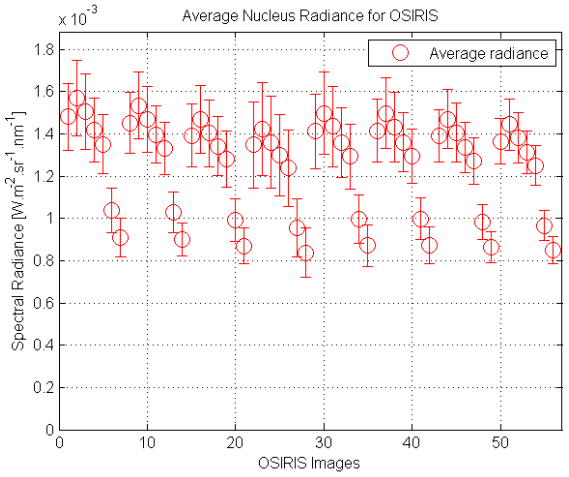

Figure 2. Average comet nucleus spectral radiance L_λ for 8 sets of OSIRIS-NAC images close in time to the NAVCAM images.

For each of the sets of OSIRIS-NAC images, we fitted a third-degree polynomial to the radiance data points in the different filters in order to obtain the spectral radiance distribution $L_O(\lambda)$. Then, we computed the average spectral radiance L_N^* in the NavCam filter band with the NavCam spectral sensitivity curve $S_N(\lambda)$ as follows:

$$L_N^*(\lambda) = \frac{\int_\lambda L_O(\lambda) S_N(\lambda) \lambda d\lambda}{\int_\lambda S_N(\lambda) \lambda d\lambda} \quad (1)$$

In Figure 2 we show the average comet nucleus spectral radiance as a function of wavelength for the first set of images (OSIRIS at T = 11:50:15 h and NavCam at T = 12:07:17 h). The circles represent the OSIRIS-NAC images whereas triangles represent the NavCam radiance calculated with equation (1) from the spectral radiance distribution derived from the calibrated OSIRIS-NAC images.

As a final step, the NavCam radiometric calibration factor *Cal* resulting from the cross-calibration exercise can be determined as the ratio of the average spectral radiance L_N^* calculated from equation (1) and the measured average come nucleus signal in DNs^{-1}:

$$Cal = \frac{L_N^*(\lambda)}{DN/s} \quad (2)$$

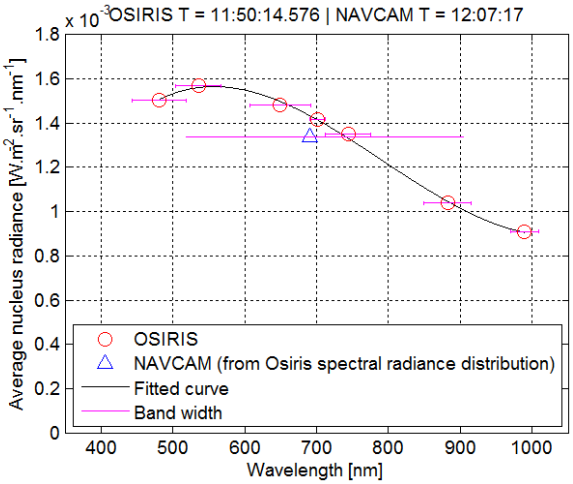

Figure 3. Average comet nucleus spectral radiance as a function of wavelength.

Table 2 summarises the L_N^* values for each of the NAVCAM images (refer to Table 1 for the image file name) as determined from the corresponding set of OSIRIS-NAC images, and the resulting NAVCAM calibration factors in $Wm^{-2}sr^{-1}nm^{-1}$/ (DNs^{-1}).

Table 2. Average comet nucleus radiances for NAVCAM images as estimated with equation (1) and the corresponding calibration factor value for each NAVCAM image.

L_N^* [$Wm^{-2}sr^{-1}nm^{-1}$]	Cal [$Wm^{-2}sr^{-1}nm^{-1}/(DNs^{-1})$]
$1.339 \cdot 10^{-3}$	$7.133 \cdot 10^{-7}$
$1.317 \cdot 10^{-3}$	$7.063 \cdot 10^{-7}$
$1.264 \cdot 10^{-3}$	$7.167 \cdot 10^{-7}$
$1.223 \cdot 10^{-3}$	$7.115 \cdot 10^{-7}$
$1.280 \cdot 10^{-3}$	$7.277 \cdot 10^{-7}$
$1.282 \cdot 10^{-3}$	$7.157 \cdot 10^{-7}$
$1.260 \cdot 10^{-3}$	$7.051 \cdot 10^{-7}$
$1.238 \cdot 10^{-3}$	$7.145 \cdot 10^{-7}$

Taking the average of the values obtained for each of the NavCam images results in a radiometric calibration factor of:

$$Cal = (7.14 \pm 0.07) \cdot 10^{-7} \frac{Wm^{-2}sr^{-1}nm^{-1}}{DNs^{-1}}. \quad (3)$$

As these images were acquired in attenuated cover position (FOC_ATT) and HIGH gain, the estimated factor is suitable for that specific mode of operation.
Therefore, in order to convert the NavCam DN counts into spectral radiance values (in $Wm^{-2}sr^{-1}nm^{-1}$), the procedure is the following:

$$L_N = Cal \frac{I_0 - Bias}{T_e} \quad (4)$$

Where I_0 is the NavCam image in DN counts, *Cal* is the radiometric calibration factor, T_e is the integration time and *Bias* is the proper bias field chosen according to the gain settings applied.

3. SPECTRAL RADIANCE PROPERTIES

Next, we have used the radiometric calibration factor to convert an extended set of NavCam images acquired at different phase angles from DNs to spectral radiance over the nucleus and studied its phase angle dependence.

We built a catalogue with 594 NavCam images acquired in FOC_ATT/HIGH mode between 2014-07-20 at 06:58:03h and 2014-08-22 at 08:07:18h. The uncalibrated images are contained in the MTP005 and MTP006 datasets available in the PSA [5]. From the initial set, we excluded 36 images which were incomplete or in which the nucleus was not completely framed. As a result, we ended up with 558 processed scenes. The phase angle α ranged from ~1º to ~55º and the spacecraft-comet distance ranged from ~6000 km to ~50 km during the considered period.

Figure 4 shows the average comet nucleus spectral radiance L_λ versus phase angle α.

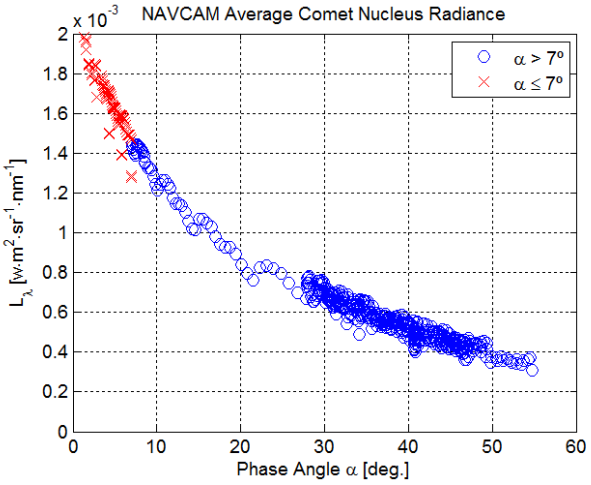

Figure 4. Average comet nucleus radiance for NavCam images.

As one can see in Figure 4, the radiance increases strongly due to the opposition effect as the phase angle decreases towards 0°. Some of the data points for $\alpha \leq 7°$ are slightly below the trend, showing smaller values for L_λ. This is due to the very small size of the comet nucleus with dimensions such as ~15 x 15 pixels at the large spacecraft-comet distances when these images were taken between July 20 and 22. Masking and point spread function issues then affect a large fraction of pixels at the border of the nucleus images. The variability at phase angles between roughly 10 and 27 degrees is due to the rotation of the comet in the corresponding image sequence. It is an indicator of spatial variability at large scales, but it can also be partially caused by shadowing effects. Due to the peculiar shape of the nucleus the extent of the shadows depends strongly on the side of the comet visible from the spacecraft. With increasing phase angle, shadows become more important and more difficult to account for in the masking process. Nevertheless, the relatively small dispersion of the data points at phase angles larger than 30 degrees (corresponding to many comet rotations) shows that the applied method is still reliable for determining characteristic radiometric properties.

4. CONCLUSION

In order to radiometrically calibrate the *Rosetta* NavCam, we carried out a cross-calibration analysis based on OSIRIS-NAC data. The best data set identified for that purpose consists of sequences of images acquired by both cameras on 2014 August 1 shortly before close encounter with the comet. The estimated radiometric factor was $(7.14 \pm 0.07) \cdot 10^{-7}$ and it is suited for processing images acquired with the attenuation filter (FOC_ATT) and HIGH gain mode. The factor will allow the conversion of NavCam DN values into radiance values in ($Wm^{-2}sr^{-1}nm^{-1}$).

6. REFERENCES

[1] Keller, H. U.et al., "OSIRIS-The Scientific Camera System onboard Rosetta". Space Science Reviews, 128, 433-506, 2007.

[2] Sierks, H. et al., "On the Nucleus Structure and Activity of Comet 67P/Churyumov-Gerasimenko". Science, 347, aaa1044, 2015.

[3] Feldman, P. et al., "Measurements of the near-nucleus coma of comet 67P/Churyumov-Gerasimenko with the Alice far-ultraviolet spectrograph on Rosetta", Astronomy and Astrophysics, 582, A8, 2015.

[4] Vincent, J. B. et al., "Summer fireworks on comet 67P". MNRAS, 462, S184-S194, 2016.

[5] Geiger, B., Barthelemy, M., "ROSETTA ORBITER NAVCAM PRELANDING MTP006, RO-C-NAVCAM-2-PRL-MTP006-V1.0", ESA Planetary Science Archive and NASA Planetary Data System, 2015. Available at ftp://psa.esac.esa.int/pub/mirror/INTERNATIONAL-ROSETTA-MISSION/NAVCAM/

[6] Otsu, N., "A threshold selection method from gray-level histograms". IEEE Transactions on Systems, Man and Cybernetics, 9, 62-66, 1979.

[7] Statella, T., Geiger, B., "Cross-calibration of the Rosetta Navigation Camera based on images of the 67P comet nucleus", MNRAS, 469, S285-S294, 2017.

[8] Tubiana, C., et al., "Scientific assessment of the quality of OSIRIS images", Astronomy and Astrophysics, 583, A46, 2015.

[9] Gutierrez-Marques, P., Sierks, H. and the OSIRIS Team, "ROSETTA ORBITER PRELANDING OSINAC 3 RDR DATA MTP 006 V1.0, RO-C-OSINAC-3-PRL-67PCHURYUMOV-M06-V1.0", ESA Planetary Science Archive and NASA Planetary Data System, 2015.